INTERNATIONAL JOURNAL FOR NUMERICAL AND ANALYTICAL METHODS IN GEOMECHANICS, VOL. 20, 847–864 (1996)

A TIME-STEPPING FINITE ELEMENT METHOD FOR ANALYSIS OF CONTAMINANT TRANSPORT IN FRACTURED POROUS MEDIA

C. J. LEO* AND J. R. BOOKER

Centre for Geotechnical Research, University of Sydney, NSW, Australia

SUMMARY

This paper describes the development of a finite element method for analysing contaminant transport in double-porosity geomaterials using a time-stepping approach. In many cases, double-porosity models may be used to represent fractured rock formations and fissured soils. A distinctive feature of utilizing this kind of model is that it is not necessary to have an intimate knowledge of the nature, distribution and properties of individual fractures and fracture arrangement since the fracture geometry and details are considered only in an averaged or equivalent continuum sense. The flux exchange that occurs between the fluid in the fractures and in the solid matrix is represented by a linear heriditary process. This has the consequence that in order to carry the solution forward from time t to $t + \Delta t$, it is necessary to know and to store the complete contaminant history up to time t. This paper shows that all the hereditary information necessary to carry the solution forward is contained in the values of certain hereditary variables at time t so that it is not necessary to store the complete time history and consequently a more efficient numerical process can be developed.

KEY WORDS: finite element-method; contaminant migration; fractured porous media; mass transport; double-porosity model

INTRODUCTION

Fissures and fractures occur widely in both soils and rocks. In soils shrinkage cracks often develop under dry and dehydrating conditions while fractures and cracks are also commonly induced in rock formations due to changes in stress conditions. The presence of a network of fissures and fractures will have significant effect on the manner in which contaminants are transported in the soil or rock. This will usually require a different technique of analysis to that used to analyse intact material. The theory of flow and mass transport in fractured media has been dealt with using a variety of approaches. Sudicky and McLaren[1] summarised the approaches used into the following broad categories: (i) equivalent non-fractured continuum, (2) discrete fracture, and (3) double porosity continuum.

In the first category, the approach is to consider an equivalent non-fractured (single continuum) model of the fractured porous medium (e.g. References 2–5). Before this type of model can be applied in an actual field situation, it is essential to know the equivalent hydraulic and transport properties representing the actual fractured formation. It has been suggested that in most practical cases, these properties must be obtained from field tests by analysis of breakthrough curves. This approach is deemed to be reasonable if the density of the fractures is very high or if the plume in consideration is very large relative to the spacings of the fractures.

* Present address: University of Western Sydney (Nepean), P.O. Box 10, Kingswood, 2747, NSW, Australia

CCC 0363–9061/96/120847–18

Received 18 August 1995
Revised 26 April 1996

For the second category, the fractures are considered discretely. In the case of a single fracture or a system of equally spaced parallel fractures in one direction, Neretnieks[6], Grisak and Pickens,[7] Tang *et al.*[8] Sudicky and Frind[9] and Ramuson[10] had been able to obtain analytical or semi-analytical solutions of mass transoprt by combining advective–dispersive transport in the fractures with diffusive transport in the solid matrix blocks. Germain and Frind[11] and Sudicky and McLaren[1] solved the mass transport problem for more complicated geometries using finite element techniques. The earlier considered only diffusive transport and the latter considered combined advective–dispersive transport in the solid matrix blocks. A drawback of this approach is that it is not always possible to know intimately the details of the fractures within the porous media and the computational costs for a system containing a large number of fractures is prohibitive.

A third approach is to assume that the fractured rocks or fissured soil behave like a double-porosity material consisting of two interacting continua each having its own properties. If the fractured system is viewed as consisting of matrix blocks separated by fissures or fractures, the continuum consisting of the matrix blocks of soil or rock, is said to have the primary porosity. The network of cracks, fractures and fissures then constitute the other continuum, this is said to have the secondary porosity. Flux transfer between the two interacting continua is represented by a source/sink term in the governing equation.

The representation of the source/sink term is necessarily complex since the distribution of the contaminant within the intact material, viz., the matrix blocks, depends on the time history of the concentration of the contaminants within the fissure system. This implies that its behaviour is hereditary in nature. For relatively simple geometries and uniform flows it is often much easier to deal with this type of behaviour in Laplace transform space (with respect to time) to the extent that most of the published analytical and numerical methods[6,8,9,12–15] have adopted this approach. It may be noted here that simple cases of the double-porosity models: a single fracture or a system of equally spaced single fractures in one direction, are in fact also discrete fracture models. Many treatments of the double porosity model idealize the actual block shapes which occur in the physical environment and replace them with regular matrix blocks of different shapes and geometries so as to lead to a mathematically tractable problem. This paper, however, outlines a different approach which does not involve the use of Laplace transform techniques but which entails a time-stepping approach and so is more able to deal with the complex geometrical configurations, distribution of properties and flows which occur in many practical situations. The double-porosity model adopted in this paper can be generated either from experimental data obtained in the laboratory or the field or from theoretical considerations.

DOUBLE-POROSITY MEDIA

As indicated above, the behaviour of many geomaterials which contain defects such as fractures, joints and collapse cavities cannot be adequately modelled using the conventional approach which were developed to deal with a non-fractured or non-fissured material. This is firstly because consideration must be given to the contaminant dispersion within the fractures, the extent of which is directly related to the magnitude of the fracture seepage velocity and the secondary porosity and, secondly, because diffusion into the primary intact matrix blocks has a significant attenuating effect on the extent of contaminant transport. Both these processes may, however, be accounted for by using a double-porosity model where the primary and secondary interacting continua are coupled by assuming that a flux exchange occurs between the two, viz., the diffusion of the contaminant into and out of the matrix blocks from within the fractures.

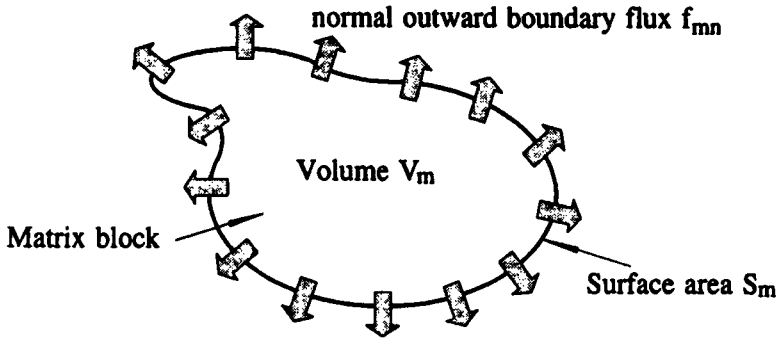

Figure 1. Schematic of matrix block and outward normal flux f_{min}

Shown in Figure 1 is the flux transfer, represented by the outward boundary flux f_{mn}, between the contaminants within the fractures and in the matrix block of some arbitrary shape where S_m denotes the surface area and V_m its volume. The 'block' need not necessarily represent a single solid matrix block of a particular shape but may be considered conceptually as comprising all disjointed pieces of matrix material in a representative elementary volume.[16,12] In this case, V_m and S_m represent the total volume and surface area, respectively, within the representative volume. If the source/sink mechanism can be assumed to be a linear hereditary process function which characterizes the transfer of flux between matrix and fracture system then it follows from the Boltzmann superposition principle that

$$\dot{q}(t) = c_f(0)\eta(t) + \int_0^t \eta(t-\tau)\frac{\partial c_f(\tau)}{\partial \tau}\mathrm{d}\tau. \tag{1}$$

where $c_f(t)$ represents the contaminant concentration in the fractures at time t, $\eta(t)$ represents the rate of contaminant diffused into the matrix for a unit increase in fracture concentration occurring at $t = 0$ and thereafter remaining constant (i.e. when $c_f(t) = H(t)$, the Heavyside function) and $\dot{q}(t)$ represents the rate of contaminant diffused into the matrix per unit volume when the fracture concentration varies with time.

Mass transport within the block will be assumed to be mainly through diffusion. For a specified matrix block, $\dot{q}(t)$ may be obtained by integrating the boundary flux flowing out of the matrix block over the block surface, i.e.

$$\dot{q}(t) = -\frac{\int_{S_m} f_{mn}\,\mathrm{d}A}{V_m} \tag{2}$$

Equation (2) has been used to derive expressions for $\dot{q}(t)$ or $\eta(t)$ for some regular block shapes. A number of these expressions are given in the Laplace transform domain (e.g. References 12, 13 and 14).

The function $\eta(t)$ can be adequately approximated in many cases by a series of exponentials having the form

$$\begin{aligned}\eta(t) &= \sum_{k=1}^{m} \eta_k \\ &= \sum_{k=1}^{m} A_k \mathrm{e}^{-\alpha_k t}\end{aligned} \tag{3}$$

where A_k, α_k are the coefficients of the exponential series. For example, the expression $\eta(t)$ for rectangular block shapes developed by Rowe and Booker[13,15] may be expressed as an infinite series of exponentials (see Appendix I). Usually, an adequate approximation can be made by taking the number of terms, m, sufficiently large. In practice, however, it is not desirable to take m too large since the storage requirement to record all the necessary information become excessive. It is helpful to provide an example of the nature of $\dot{q}(t)$ displayed in graphical form since the discussion up to this stage has been fairly abstract. In Appendix II, two examples of this function is presented, for the cases when $c_f(t) = H(t)$ and $c_f(t) = t$.

It is perhaps also worth remarking that the double-porosity model may also be used to model non-fissured geomaterials by the simple device of assuming that the flux transfer of the term $\dot{q}(t)$ vanishes completely. The approach thus provides a method which is able to take account of different regions with different properties, different flow regimes and different degrees of fissuring (including no fissuring).

EQUATIONS OF CONTAMINANT TRANSPORT

Since it is assumed that fracture locations and arrangements need not be accurately mapped and only the properties in an averaged sense are utilized, the mass balance equation of contaminant transport may be described by the following partial differential equation:

$$\nabla\cdot(\mathbf{D}_a\nabla c_f) - \nabla\cdot(\mathbf{V}_a c_f) = n_f\frac{\partial c_f}{\partial t} + g + \dot{q} \tag{4}$$

where $\nabla = (\partial/\partial x,\ \partial/\partial y,\ \partial/\partial z)^T$ is the gradient operator in Cartesian (x, y, z) space; c_f is the concentration of the contaminant in the fractures, n_f the effective porosity of the fractures (the secondary porosity) within the fracture–matrix system, $\mathbf{D}_a$ the hydrodynamic dispersion tensor in the fracture system, $\mathbf{V}_a$ the vector of the components of the Darcian ground water velocity; g the sum of the rates at which contaminant is adsorbed on to the fracture walls per unit volume and contaminant decay, and $\dot{q}$ the rate at which the contaminant migrates from the fractures into the matrix per unit volume.

Scheidegger[17] and Bear[18] have shown that the coefficients of hydrodynamic dispersion is a function of the velocity in the fractures and can be assumed to be given by

$$D_{aij} = D_0\delta_{ij} + \alpha_{ijmn}\frac{V_{am}V_{an}}{V_a} \tag{5a}$$

where D_0 is the effective diffusion coefficient of the contaminant, δ_{ij} the Kronecker delta, V_{am} the components of the Darcian ground water velocity in the fractures, V_a the magnitude of the Darcian ground water velocity in the fractures, and α_{ijmn} the components of the longitudinal dispersivity tensor.

In isotropic soil the dispersivity tensor only depends on two independent components, α_L the longitudinal dispersivity in the direction of flow and α_T the transverse dispersivity orthogonal to the direction of flow so that $\mathbf{D}_a$ is given by

$$D_{aij} = (D_0 + \alpha_T V_a)\delta_{ij} + (\alpha_L - \alpha_T)\frac{V_{ai}V_{aj}}{V_a}. \tag{5b}$$

The term g comprises the rate of contaminant decay g_D and the rate of adsorption onto the fracture walls g_A, i.e.

$$g = g_A + g_D \tag{6a}$$

where

$$g_D = n_f \gamma_f c_f \tag{6b}$$

and γ_f is the decay constant of the contaminant. The rate of adsorption onto the fracture walls may be assumed to have the general form

$$g_A = g_A\left(c_f, \frac{\partial c_f}{\partial t}\right) \tag{6c}$$

When the concentration is low, the following relationship[18] is often used:

$$g_A = \beta_f K_{df} \frac{\partial c_f}{\partial t} \tag{6d}$$

where K_{df} is the distribution coefficient defined as the mass of solute adsorbed per unit area of surface divided by the concentrations of contaminant in the solution and β_f represents the surface area per unit volume. Instead of explicitly expressing the contaminant decay and adsorption as a distinct term 'g' as represented above, it can alternatively be included into the expression for '$\dot{q}$' which has a relationship defined by equation (1). This approach proves to be particularly useful when the double-porosity parameters are determined experimentally since all the terms may be 'lumped' together.

Using equations (1), (3), (4) and (6), the governing equation for mass transport within the fractures can be expressed in the form:

$$\int_0^t \{\nabla\cdot(\mathbf{D}_a \nabla c_f) - \nabla\cdot(\mathbf{V}_a c_f)\}\,d\tau = (n_f + \beta_f K_{df})(c_f - c_f(0)) + \int_0^t n_f \gamma_f c_f\,d\tau + q(t) \tag{7}$$

where it is assumed that parameter γ_f is adjusted to account for decay of both adsorbed and nonadsorbed contaminant and where it follows from equation (1) that

$$q(t) = \int_0^t \eta(t-\tau) c_f(\tau)\,d\tau \tag{8}$$

FINITE ELEMENT APPROXIMATION

In the finite element process, it is intended to seek an approximation within each element of the finite element mesh which has a form defined by

$$c_f \approx \hat{c}_f = \sum_1^k N_j^{(e)} c_{fj}^{(e)} = [\mathbf{N}^{(e)}]\mathbf{c}_f^{(e)} \tag{9}$$

where $[\mathbf{N}^{(e)}]$ is the assumed matrix of element shape functions prescribed in terms of the independent variables (such as the coordinates, x, y, z; Reference 20) and $\mathbf{c}_f^{(e)}$ is the vector of the nodal concentrations within the fracture. In equation (9) and subsequent equations, the superscript 'e' will be used to indicate that the indicated quantity is associated with element e. The Galerkin method can be used to write an element domain integral equation of (7) which has been weighted by the shape functions so that

$$\int_0^t \int_{V^{(e)}} [\mathbf{N}^{(e)}]^T \{\nabla\cdot(\mathbf{D}_a^{(e)}\nabla\hat{c}_f) - \nabla\cdot(\mathbf{V}_a^{(e)}\hat{c}_f)\}\,dV^{(e)}\,d\tau = \int_0^t \int_{V^{(e)}} [\mathbf{N}^{(e)}]^T n_f^{(e)} \gamma_f \hat{c}_f\,dV^{(e)}\,d\tau$$

$$+ \int_{V^{(e)}} [\mathbf{N}^{(e)}]^T \{(n_f^{(e)} + \beta_f^{(e)} K_{df}^{(e)})(\hat{c}_f - \hat{c}_f(0)) + q^{(e)}\}\,dV^{(e)} \tag{10}$$

where $V^{(e)}$ is the domain of element e.

It may be observed at this stage that if equation (8) is introduced into equation (10) that it will be necessary to store the entire time history of each nodal concentration. For this reason $q^{(e)}$ is now assumed to be approximated using a finite series of the type described by equation (3), viz.,

$$\begin{aligned} q^{(e)} \approx \hat{q}^{(e)} &= \sum_{l}^{m} \hat{q}_k^{(e)} \\ &= \sum_{l}^{m} \int_0^t \eta_k^{(e)}(t-\tau) c_f(\tau)\, d\tau \end{aligned} \tag{11}$$

Furthermore, if it is assumed that the function $\eta^{(e)}(t)$ may be approximated by an exponential series shown in equation (3) then $\hat{q}_k^{(e)}$ is found to satisfy the partial differential equation,

$$\frac{\partial \hat{q}_k^{(e)}}{\partial t} + \alpha_k^{(e)} \hat{q}_k^{(e)} = A_k^{(e)} \hat{c}_f \tag{12}$$

where $\hat{q}_k^{(e)}\ (t = 0) = 0$.

It is worth mentioning that the number of terms, m, necessary to capture the essential behaviour may be reduced to a minimum by applying curve-fitting methods that have already been developed (e.g. Reference 21).

After integrating by parts and applying the divergence theorem, equation (12) leads to a system of algebraic equations which may be written as

$$\int_0^t \{[\mathbf{M}^{(e)} + n_f^{(e)} \gamma_f \mathbf{A}^{(e)}] \mathbf{c}_f^{(e)}\}\, d\tau + \mathbf{F}^{(e)} = 0 \tag{13}$$

where

$$\begin{aligned} [\mathbf{M}^{(e)}] = \int_{V^{(e)}} \Bigg\{ &[\mathbf{B}^{(e)}]^T \mathbf{D}_a^{(e)} [\mathbf{B}^{(e)}] - \left[\frac{\partial \mathbf{N}^{(e)}}{\partial x}\right]^T V_{ax} [\mathbf{N}^{(e)}] - \left[\frac{\partial \mathbf{N}^{(e)}}{\partial y}\right]^T V_{ay} [\mathbf{N}^{(e)}] \\ &- \left[\frac{\partial \mathbf{N}^{(e)}}{\partial z}\right]^T V_{az} [\mathbf{N}^{(e)}] \Bigg\} dV^{(e)} \end{aligned} \tag{14}$$

$$[\mathbf{A}^{(e)}] = \int_{A^{(e)}} [\mathbf{N}^{(e)}]^T [\mathbf{N}^{(e)}]\, dV^{(e)} \tag{15}$$

$$[\mathbf{B}^{(e)}] = \begin{bmatrix} \dfrac{\partial N_1^{(e)}}{\partial x} & \dfrac{\partial N_2^{(e)}}{\partial x} & \cdots & \dfrac{\partial N_k^{(e)}}{\partial x} \\ \dfrac{\partial N_1^{(e)}}{\partial y} & \dfrac{\partial N_2^{(e)}}{\partial y} & \cdots & \dfrac{\partial N_k^{(e)}}{\partial y} \\ \dfrac{\partial N_1^{(e)}}{\partial z} & \dfrac{\partial N_2^{(e)}}{\partial z} & \cdots & \dfrac{\partial N_k^{(e)}}{\partial z} \end{bmatrix} \tag{16}$$

$$\mathbf{F}^{(e)} = \int_{V^{(e)}} [\mathbf{N}^{(e)}]^T \left\{ (n_f^{(e)} + \beta_f^{(e)} K_{df}^{(e)})(\hat{c}_f - \hat{c}_f(0)) + \sum_{l}^{m} \hat{q}_k^{(e)} \right\} dV^{(e)} \tag{17}$$

An approximation of the time integral of c_f over the time interval $(t, t + \Delta t)$ can be written as

$$\int_t^{t+\Delta t} c_f(\tau)\, d\tau \approx \Delta t \{c_f(t) + \theta \Delta c_f\} \tag{18}$$

where $\Delta c_f = c_f(t + \Delta t) - c_f(t)$ and θ is a parameter determining the integration rule ($\theta = \frac{1}{2}$ corresponds to the trapezoidal rule).

Using the approximation defined by equation (18) it is then found that

$$\Delta t[\mathbf{M}^{(e)} + n_f^{(e)}\gamma_f \mathbf{A}^{(e)}]\{(1-\theta)\mathbf{c}_f^{(e)}(t) + \theta \mathbf{c}_f^{(e)}(t+\Delta t)\}\,\mathrm{d}\tau + \Delta \mathbf{F}^{(e)} = 0 \tag{19}$$

where

$$\Delta \mathbf{F}^{(e)} = \int_{V^{(e)}} [\mathbf{N}^{(e)}]^{\mathrm{T}} \left\{ (n_f^{(e)} + \beta_f^{(e)} K_{\mathrm{df}}^{(e)}) \Delta \hat{c}_f + \sum_l^m \Delta \hat{q}_k^{(e)} \right\} \mathrm{d}V^{(e)} \tag{20}$$

The next stage in the formulation will be to find an approximation for $\Delta \hat{q}_k^{(e)}$ and this may be achieved by utilizing the partial differential equation (12). Thus, in the same manner as previously, an approximation over the time interval $(t, t + \Delta t)$ of equation (12) for element e can be written as

$$\Delta \hat{q}_k^{(e)} + \alpha_k^{(e)}\{\hat{q}_k^{(e)}(t) + \theta \Delta \hat{q}_k^{(e)}\}\Delta t = A_k\{\hat{c}_f(t) + \theta \Delta \hat{c}_f\}\Delta t \tag{21}$$

so that

$$\Delta \hat{q}_k^{(e)} = \frac{\Delta t}{(1 + \alpha_k^{(e)} \Delta t \theta)} \{A_k^{(e)}[(1-\theta)\hat{c}_f(t) + \theta \hat{c}_f(t + \Delta t)] - \alpha_k^{(e)} \hat{q}_k^{(e)}(t)\} \tag{22}$$

After substituting equation (22) into equation (20) and some rearrangements of equation (19), it is found that

$$\left\{\theta \Delta t\,[\mathbf{M}^{(e)}] + \left[\theta \Delta t\, n_f^{(e)}\gamma_f + (n_f^{(e)} + \beta_f^{(e)} K_{\mathrm{df}}^{(e)}) + \sum_{k=1}^m \frac{\theta \Delta t\, A_k^{(e)}}{(1 + \alpha_k^{(e)} \Delta t \theta)}\right][\mathbf{A}^{(e)}]\right\}\mathbf{c}_f^{(e)}(t + \Delta t)$$
$$+ \left\{(1-\theta)\Delta t\,[\mathbf{M}^{(e)}] + \left[(1-\theta)\Delta t n_f^{(e)}\gamma_f - (n_f^{(e)} + \beta_f^{(e)} K_{\mathrm{df}}^{(e)}) + \sum_{k=1}^m \frac{(1-\theta)\Delta t\, A_k^{(e)}}{(1 + \alpha_k^{(e)} \Delta t \theta)}\right][\mathbf{A}^{(e)}]\right\}\mathbf{c}_f^{(e)}(t)$$
$$+ \mathbf{H}^{(e)} = 0 \tag{23a}$$

where

$$\mathbf{H}^{(e)} = -\int_{V^{(e)}} [\mathbf{N}^{(e)}]^{\mathrm{T}} \sum_{k=1}^m \frac{\alpha_k^{(e)} \Delta t\, \hat{q}_k^{(e)}(t)}{(1 + \alpha_k^{(e)} \Delta t\, \theta)} \mathrm{d}V^{(e)} \tag{23b}$$

Equations (22) and (23) can now be 'marched forward' in time since all hereditary information needed is contained in $\hat{q}_k^{(e)}(t)$. Since $\hat{q}_k^{(e)}(t)$ may be discontinuous at the nodes, it is expedient to evaluate the integral appearing in equation (23b) using nominated values at the Gauss points of the elements. Sometimes the initial distribution of concentration will be prescribed on an element by element basis so that within each element it is convenient to assume that the initial concentration is a constant value. This clearly means that under such assumptions it is not possible to define unique nodal concentrations at $t = 0$. It is found useful to express the second term, which contains the nodal concentration vector $\mathbf{c}_f^{(e)}(t)$, in equation (23a) in an alternative form which utilizes the concentration values at the Gauss points. In this case, equation (23a) may be rewritten as

$$\left\{\theta \Delta t\,[\mathbf{M}^{(e)}] + \left[\theta \Delta t\, n_f^{(e)}\gamma_f + (n_f^{(e)} + \beta_f^{(e)} K_{\mathrm{df}}^{(e)}) + \sum_{k=1}^m \frac{\theta \Delta t\, A_k^{(e)}}{(1 + \alpha_k^{(e)} \Delta t \theta)}\right][\mathbf{A}^{(e)}]\right\}\mathbf{c}_f^{(e)}(t + \Delta t) + \mathbf{R}^{(e)} = 0 \tag{24}$$

For example, in a parallelepiped element, the last term in equation (24) may be evaluated by Gauss quadrature as

$$\mathbf{R}^{(e)} = \sum_{i=1}^{m}\sum_{j=1}^{m}\sum_{k=1}^{m} w_i w_j w_k \mathbf{r}^{(e)}(\xi_i, \eta_j, \zeta_k, t)|\mathbf{J}(\xi_i, \eta_j, \zeta_k)| \tag{25}$$

where ξ_i, η_j, ζ_k are the normalized coordinates of Gauss points along local axes, w_i, w_j, w_k the weights of the Gaussian quadrature, $|\mathbf{J}|$ is the determinant of the transform Jacobian matrix, and

$$\mathbf{r}^{(e)} = [\mathbf{N}^{(e)}]\left\{\left[(1-\theta)\Delta t n_f^{(e)}\gamma_f - (n_f^{(e)} + \beta_f^{(e)} K_{df}^{(e)}) + \sum_{k=1}^{m}\frac{(1-\theta)\Delta t A_k^{(e)}}{(1+\alpha_k^{(e)}\Delta t\theta)}\right]\hat{c}_f^{(e)} - \sum_{k=1}^{m}\frac{\alpha_k^{(e)}\Delta t\,\hat{q}_k^{(e)}(t)}{(1+\alpha_k^{(e)}\Delta t\,\theta)}\right\}$$
$$+ (1-\theta)\Delta t\left\{[\mathbf{B}^{(e)}]^{\mathrm{T}}\mathbf{D}_a^{(e)}\nabla\hat{c}_f^{(e)} - \left(V_{ax}\left[\frac{\partial\mathbf{N}^{(e)}}{\partial x}\right]^{\mathrm{T}} + V_{ay}\left[\frac{\partial\mathbf{N}^{(e)}}{\partial y}\right]^{\mathrm{T}} + V_{az}\left[\frac{\partial\mathbf{N}^{(e)}}{\partial z}\right]^{\mathrm{T}}\right)\hat{c}_f^{(e)}\right\}.$$

After assembly of the elements, the global system of algebraic equations will appear in the form as follows:

$$[\mathbf{M} + \mathbf{A}]\{\mathbf{c}_f(t + \Delta t)\} = \mathbf{R} \tag{26}$$

where $[\mathbf{M} + \mathbf{A}]$ is an asymmetrical matrix and $\mathbf{R}$ is the known right-hand-side vector which is a function of the dependent variable at time level t. Equation (26) thus enables the values of the nodal concentration at the next time level $(t + \Delta t)$ to be determined and the values of $\hat{q}_k^{(e)}(t)$ may be updated to the next time level using equation (22).

RESULTS

Benchmarking problems

In this section, the results of the finite element method will be compared against other analytical and numerical solutions The aim of this exercise is to verify, at least in some respects, the validity and accuracy of the finite element solutions. Two test problems are described below.

Test Problem 1. The first benchmarking problems is a one-dimensional case which involves a surface landfill overlying a deep layer of fractured soil with parallel fracture planes in the vertical direction (the full expression of η is given in Appendix I). One-dimensional contaminant transport from a surface landfill into fractured material had been examined earlier by Rowe and Booker[13,14] utilizing a semi-analytic approach which solved the problem in the Laplace transform space and then obtained the solutions in time domain by numerically inverting the Laplace transform solutions using a very accurate inversion algorithm due to Talbot.[22] In the finite element analysis, a rectangular mesh of 48 quadrilateral elements was created, the first 16 elements were then prescribed an initial concentration value $c/c_0 = 1$ while the remaining elements were prescribed identically zero concentration. The elements prescribed with an initial concentration simulate the presence of the contaminant in the landfill at time $t = 0$. It may be observed that the prescription of an initial concentration for the appropriate elements in the mesh provide a convenient method enabling a landfill, contaminated source or a contaminated zone to be represented in the analysis. In this way, initially contaminated elements may be utilized to represent contaminated zones of virtually any geometry or shape.

A Darcian ground water velocity of 0·004 m/a is assumed to be flowing uniformly downwards in this problem, and the contaminant is assumed to be conservative and non-radioactive. The properties of the fractures and soil are shown in Table I(a) where H_1 represents the half-spacing of

Table I(a). Properties of fractures and solid matrix in problem 1

D_0 (m²/a)	α_L (m)	$\beta_f K_{df}$	n_f	D_m (m²/a)	n_m	H_1 (m)
0·01	1·0	0	0·1	0·01	0·1	1

Table I(b). Coefficients of A_k and α_k used in the exponential series of test problem 1

k	1	2	3	4	5	6	7
A_k	0·002	0·002	0·002	0·002	0·002	0·002	0·002
α_k	0·02467	0·2221	0·6170	1·2090	1·9986	2·9856	4·1700

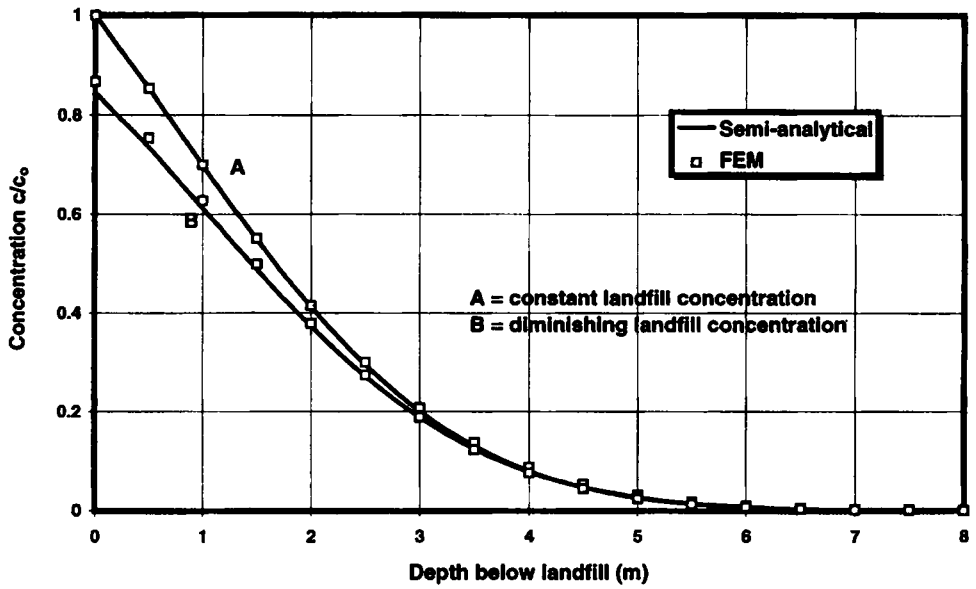

Figure 2. FEM vs. semi-analytical solutions for one-dimensional problem at 40 yr

the vertical fracture planes, n_m is the molecular diffusion coefficient in the solid matrix and n_m the porosity of the matrix (see Appendix I). Although η is an infinite exponential series, in practice, fewer than 10 terms were required to approximate adequately the series in most cases and in this problem 7 terms were used (Table I). Results at $t = 40$ yr shown in Figure 2 indicate that the finite element solutions compare very well with the solutions using the method of Rowe and Booker.[13,14]

Test Problem 2. The second problem examines a long waste trench (20 m × 5 m cross-section) placed in a 8 m deep soil layer which is fissured and bounded by upper and lower surfaces which are impermeable. The properties in the non-fractured waste zone and the surrounding fractured medium are presented in Table II(a) where it is to be noted that the notations used represent either fractured or non-fractured properties as appropriate. In the fractured soil layer a Darcian velocity of 0·004 m/a is flowing in the horizontal x direction and the fracture characteristics were approximated by 9 terms of the exponential series. Table II(b) gives the values of the coefficients

Table II(a). Properties in problem 2

	D_0 (m^2/a)	α_L (m)	α_T (m)	$\beta_f K_{df}$ or ρK_d	n_f or nD_m (m^2/a)		n_m	H_1 (m)	H_3 (m)
Waste zone	1·0	1·0	0·1	0	0·5	–	–	–	
Fractured zone	0·5	1·0	0·1	0	0·0006	0·003	0·1	0·1	0·1

Table II(b). Coefficients of A_k and α_k used in the exponential series of test problem 2 and illustrative example

k	1	2	3	4	5	6	7	8	9
A_k	0·09727	0·05404	0·05058	0·05404	0·01081	0·00735	0·05058	0·00735	0·00389
α_k	1·48044	7.40220	19.2457	7.40220	13.3240	25.1675	19.2457	25.1675	37.0110

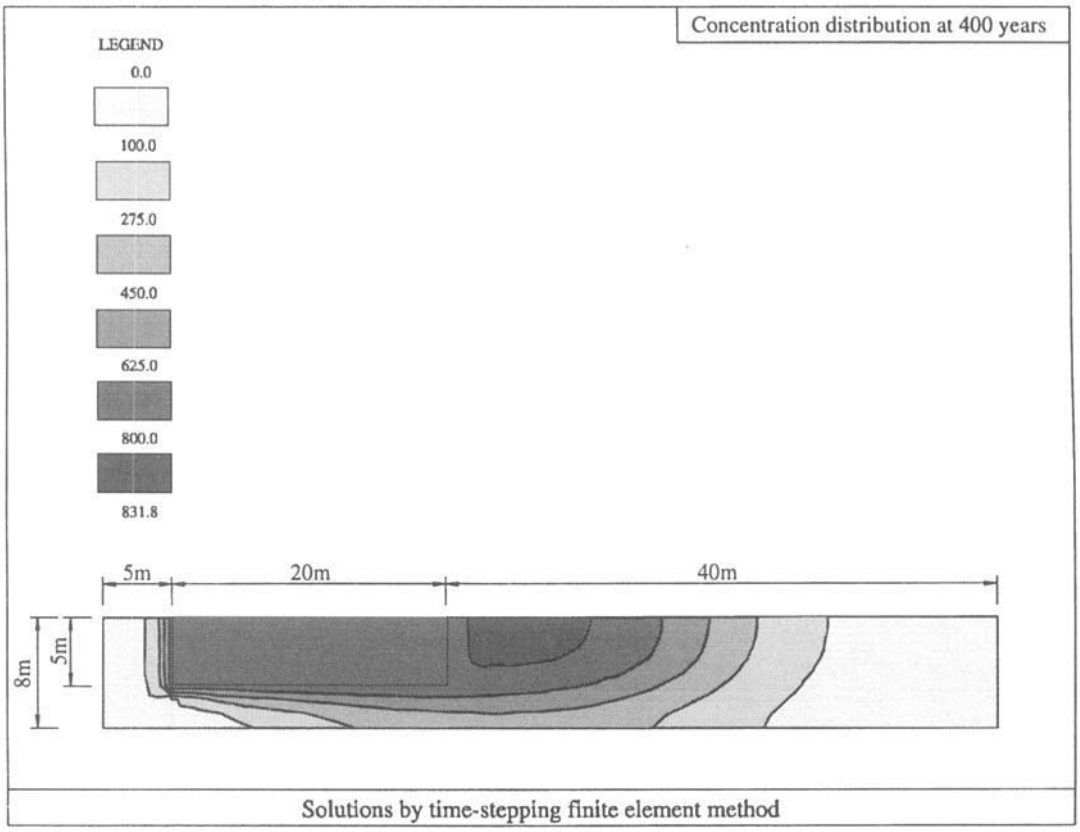

Figure 3. Contaminant distribution from time-stepping finite element method

A_k and the exponents α_k used in this problem. These values represent approximately 2 sets of orthogonal fracture planes, each with half-spacing (H_1, H_3) of 0·1 m, a matrix diffusion coefficient (D_m) of 0·003 m^2/a and a matrix porosity (n_m) of 0·1 (see Table II(a) and Appendix I). The time-stepping finite element method is employed to develop contaminant distribution for this problem at various times of interest and Figure 3 shows the results for a time $t = 400$ yr. Since

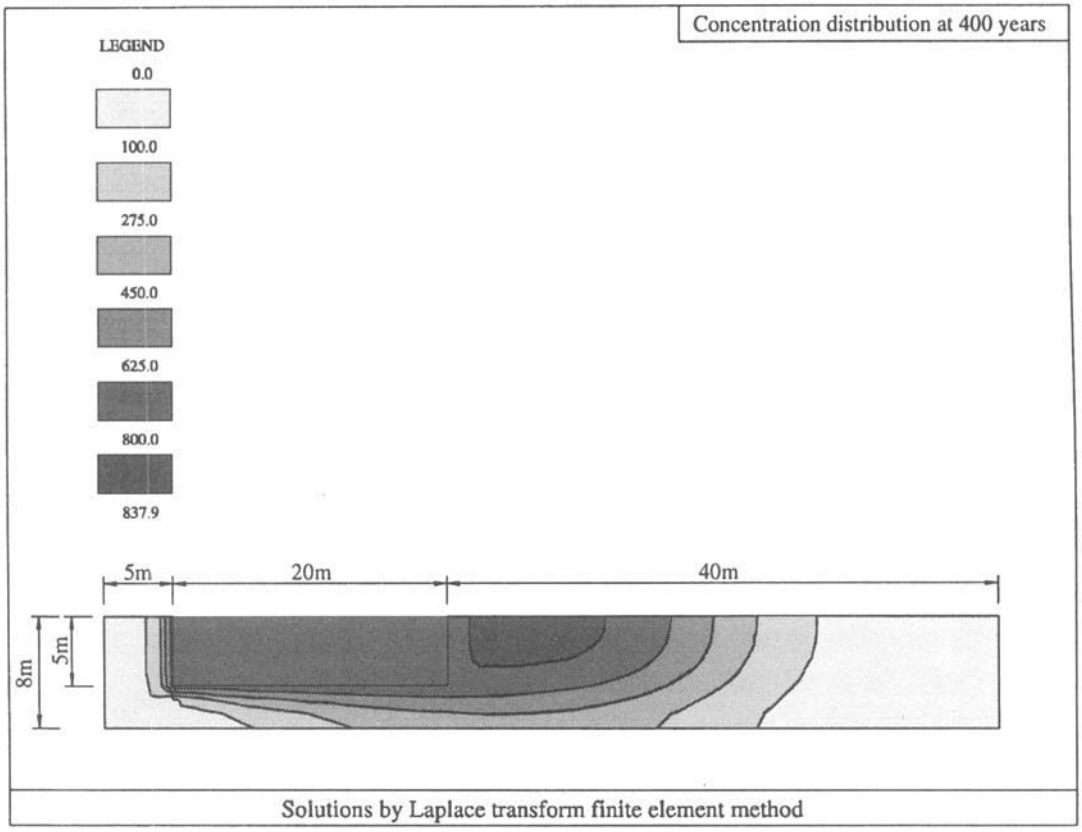

Figure 4. Contaminant distribution from Laplace transform finite element method

there is no known analytical solution for this case, an alternative Laplace transform finite element technique is used to provide a comparison. This approach applies Laplace transform techniques to eliminate the time variable t and then uses conventional finite element techniques to solve for the concentrations in space. The values of the concentration in real time are finally obtained by numerical inversion of the Laplace transform. The concentration distribution obtained in this manner is shown in Figure 4 where about 500 quadrilateral elements had been used in this analysis. The agreement in the concentration distribution shown in Figures 3 and 4 is found to be satisfactory.

Illustrative examples

The time-stepping finite element method developed in this paper was then used to study the time effects of a landfill founded in fractured media. The soil profile with a cross-section of the landfill is shown in Figure 5 where it may be observed that the fractured media consist of two 20 and 10 m thick layers interspersed by two 5 m thick sandy aquifers of very high permeability. Below the lower boundary of the lower sandy layer is an impermeable layer. The landfill has a top width of 150 m, a bottom of 90 m, a depth of 10 m and side slopes with 3H:1V gradient. It is completely filled with compacted waste producing a contaminant leachate of height 10 m and initial concentration 1000 mg/l. On the left-hand side of the rectangular domain (Figure 5),

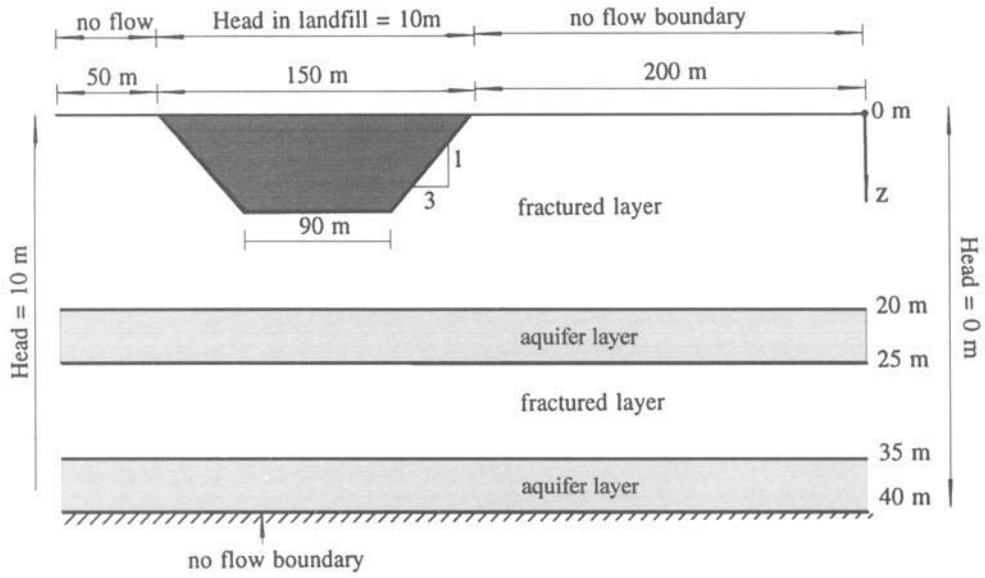

Figure 5. Schematic of landfill and media profile in illustrative example

Table III. Permeability values of soil materials in illustrative example

	K_{xx} (cm/s)	K_{zz} (cm/s)
Intact material (solid matrix)	1×10^{-4}	1×10^{-4}
Sandy soil	1×10^{-3}	1×10^{-3}

a ground water head of 10 m is present, in the landfill the head is assumed to be 10 m and the head on the right-hand side boundary is zero. For the given hydraulic conductivity listed in Table III, the steady-state flow field is computed by the finite element program FESEP[23] and is shown in Figure 6. Flow velocity is highest in the sandy materials, this is evident by comparing the magnitudes of the velocity vectors in the various media layers. The flow field surrounding the landfill is fairly complex since the velocity vector varies in direction and magnitude from point to point. Nevertheless, the potential gradient present ensures that flow occurs generally in the direction from left to right and downwards.

In this illustrative example, the properties of the waste zone and soil layers are shown in Table IV and the fracture characteristics are assumed to be represented by the parameters shown in Table II(b) the same as those used for the test example 2. The finite element mesh used in the analysis is composed of about 1500 quadrilateral elements. It may be noted that a mixture of fractured and non-fractured elements were found in the mesh; the non-fractured elements represent the landfill and the sandy layers, whereas fractured elements were utilized to represent the fractured media. Once again, the notations used in the headings in Table IV may represent either the fractured or non-fractured properties as the case may be. For example, the sorption for fractured media (β_f/K_f) is replaced by ρK_d is a non-fractured zone where ρ is the dry density of the soil and K_d is the distribution coefficient. The subscript 'f' has also been dropped from n, the porosity of the soil, to indicate that it is a non-fractured material. Figure 7(a) shows the contaminant distribution in the fractured media due to the presence of the landfill after 1 yr. It

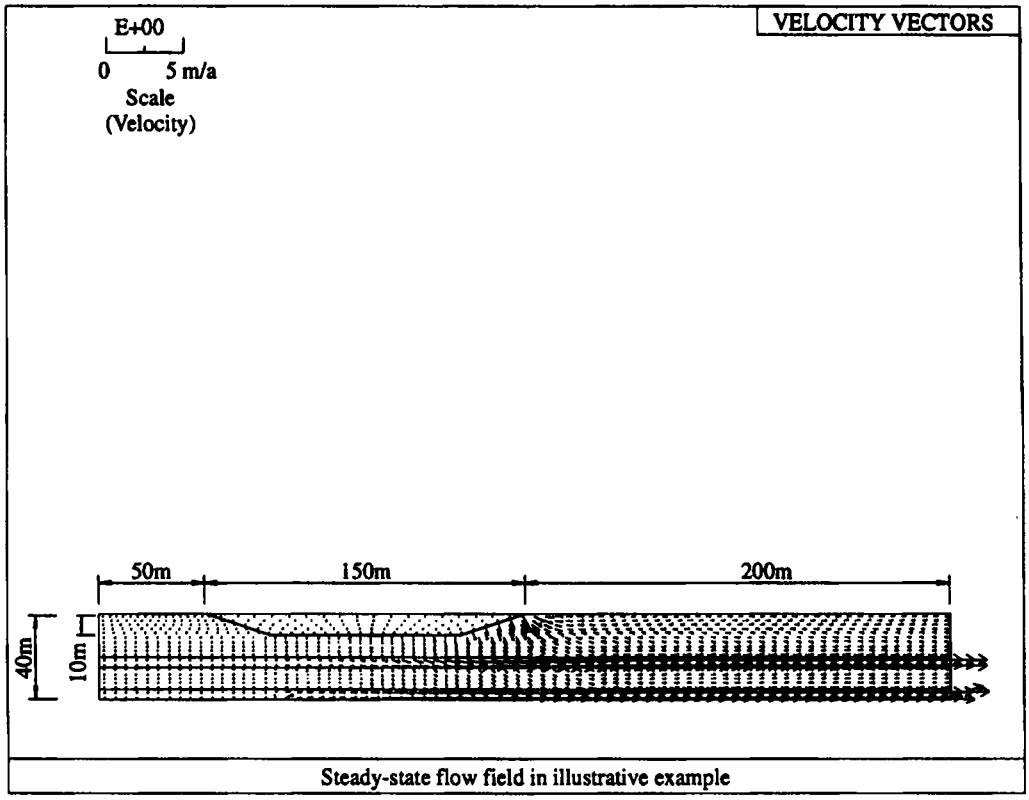

Figure 6. Steady-state flow field in illustrative example

Table IV. Properties in waste zone, fractured and aquifer layers

	D_0 (m²/a)	α_L (m)	α_T (m)	ρK_d or $\beta_f K_{df}$	n or n_f
Waste zone	10·0	0·1	0·0	0	0·5
Fractured layer	0·1	1·0	0·1	0	0·0006
Aquifer lyaer	0·1	1·0	0·1	0	0·3

may be observed that a contaminant plume of 10 mg/l is just starting to penetrate the top aquifer. After 5 yr, the plume has fully penetrated through this aquifer into the lower layer of the fractured media. In the top aquifer, the plume is transported along by the flow in the aquifer at a much faster rate than in the adjoining fractured material (Figure 7(b)). At $t = 10$ yr, the plume has penetrated into the lower aquifer (Figure 7(c)) and at this point in time, both aquifers will have become contaminated by the waste landfill.

CONCLUSIONS

This paper presents a time-stepping finite element method to model contaminant migration in double-porosity fractured materials which can be used to model the contaminant migration in regions containing both intact and fractured or fissured geo-materials having different properties.

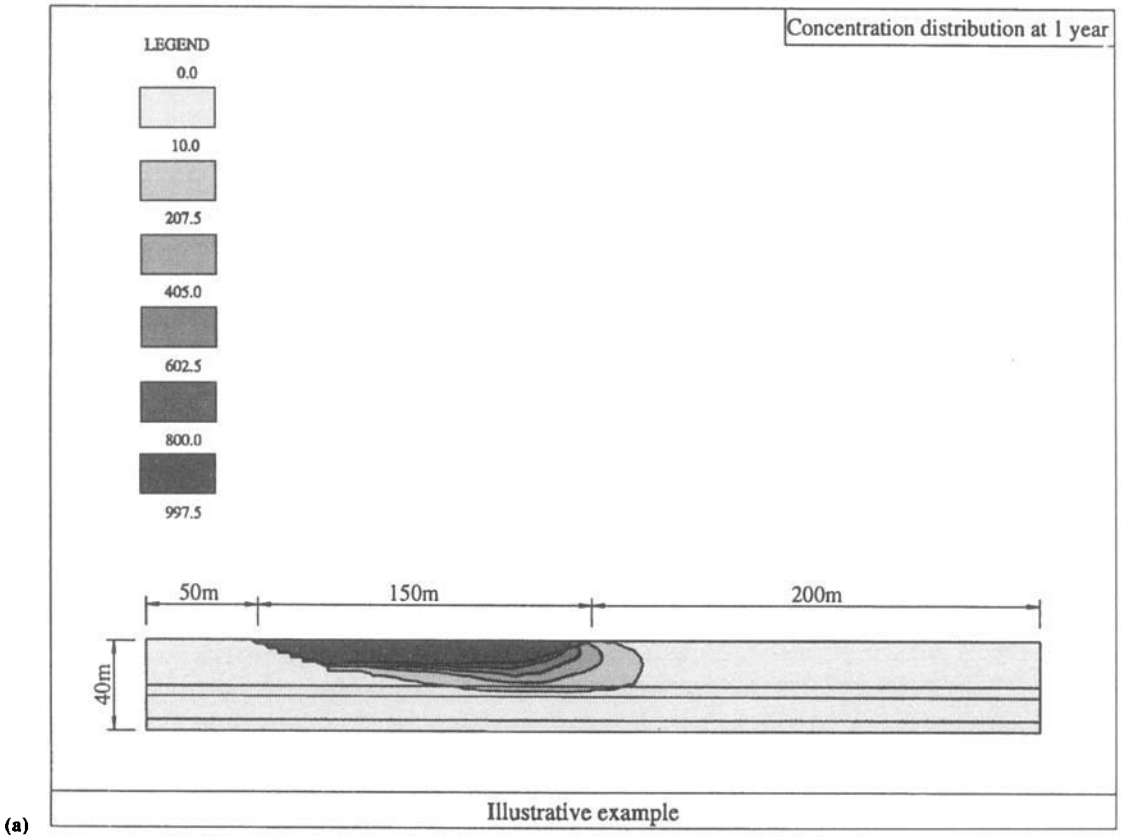

(a)

Figure 7(a). Contaminant distribution at 1 yr in illustrative example

The method involves approximating the source/sink term in the governing equation by the sum of exponentials. The coefficients in this series may be obtained either experimentally or by a theoretical approach, if the matrix blocks were regular. The model has been validated by comparison with semi-analytic and other numerical solutions and also been used to investigate the migration of contamination from a waste repository in the presence of a complex flow field.

APPENDIX I

In the papers by Rowe and Booker[13,14] they assumed that the fracture media may be idealized as consisting of matrix material separated by a system of orthogonal planar fractures as shown in Figure 8. The fracture system may consists of one, two or three sets of fractures with spacings $2H_1$, $2H_2$, $2H_3$ and effective apertures $2h_1$, $2h_2$ $2h_3$. Set 1 of the fracture planes is parallel to the y–z plane, set 2 to the z–x plane and set 3 to the x–y plane. Based on this, Rowe and Booker[13,14] derived expressions of η for the matrix blocks which are slabs (i.e. one set of parallel fracture planes), infinitely long rectangular blocks (two sets of parallel fracture planes) and rectangular blocks (three sets of parallel fracture plane). These expressions are given in Laplace transform space but may be inverted to obtain the corresponding analytical solutions given below.

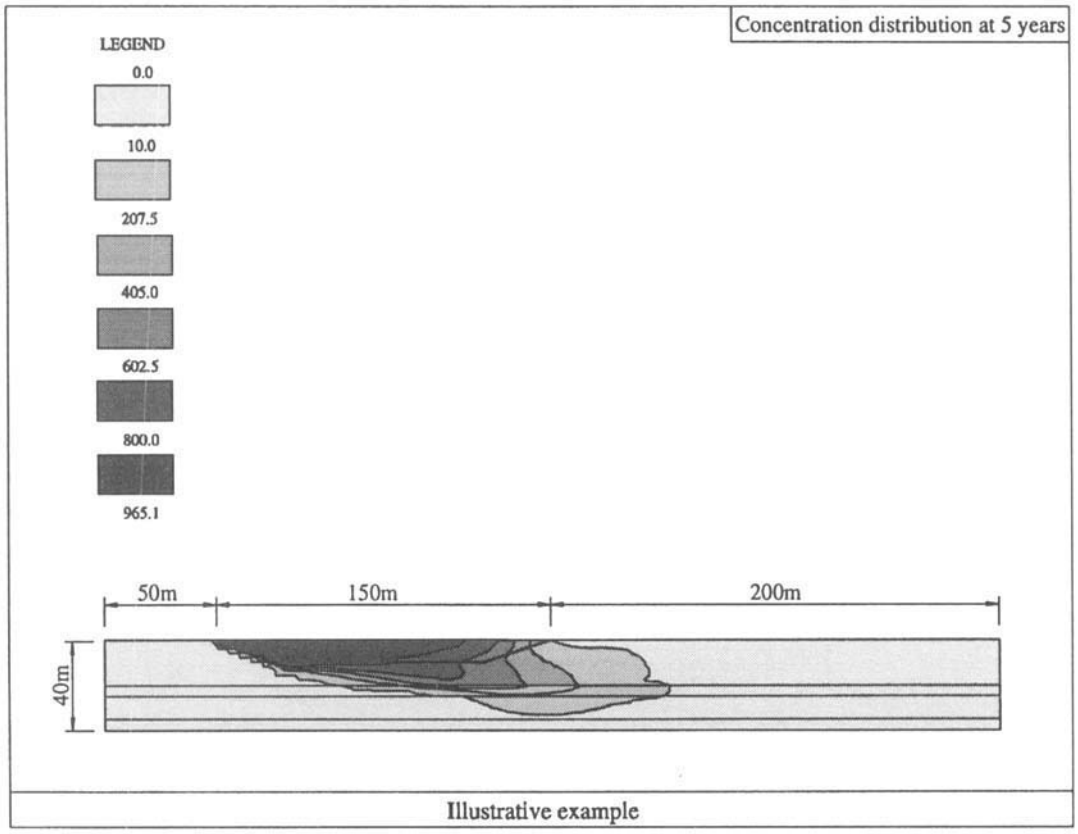

(b)

Figure 7(b). Contaminant distribution at 5 yr in illustrative example

For a slab, the analytical expression is

$$\eta = \frac{2n_m D_m}{H_1^2} \sum_{j=1}^{\infty} \exp\left(-\left(\frac{\gamma_m}{R_m} + \kappa_j^2 \frac{D_m}{R_m} \right) t \right) \tag{27}$$

where $\kappa_j = (j - 1/2)\pi/H_1$; n_m is the porosity of solid matrix, D_m the diffusion coefficient of contaminant in the solid matrix of intact material in fractured zone, R_m the $(1 + \rho_m K_d/n_m)$, the retardation coefficient in the solid matrix, ρ_m the dry density of the solid matrix, K_m the distribution coefficient in the matrix, and γ_m the decay constant of contaminant in the solid matrix.

For an infinitely long rectangular block,

$$\eta = 4n_m D_m \sum_{j=1}^{\infty} \sum_{l=1}^{\infty} \frac{(\kappa_j^2 + \omega_l^2)}{((\kappa_j H_1)^2 (\omega_l H_3)^2)} \exp\left(-\left(\frac{\gamma_m}{R_m} + \frac{D_m}{R_m}(\kappa_j^2 + \omega_l^2) \right) t \right) \tag{28}$$

where $\omega_l = (l - 1/2)\pi/H_3$. For a rectangular block,

$$\eta = 8n_m D_m \sum_{j=1}^{\infty} \sum_{k=1}^{\infty} \sum_{l=1}^{\infty} \frac{(\kappa_j^2 + \mu_k^2 + \omega_l^2)}{((\kappa_j H_1)^2 (\mu_k H_2)^2 (\omega_l H_3)^2)} \exp\left(-\left(\frac{\gamma_m}{R_m} + \frac{D_m}{R_m}(\kappa_j^2 + \mu_k^2 + \omega_l^2) \right) t \right) \tag{29}$$

where $\mu_k = (k - 1/2)\pi/H_2$.

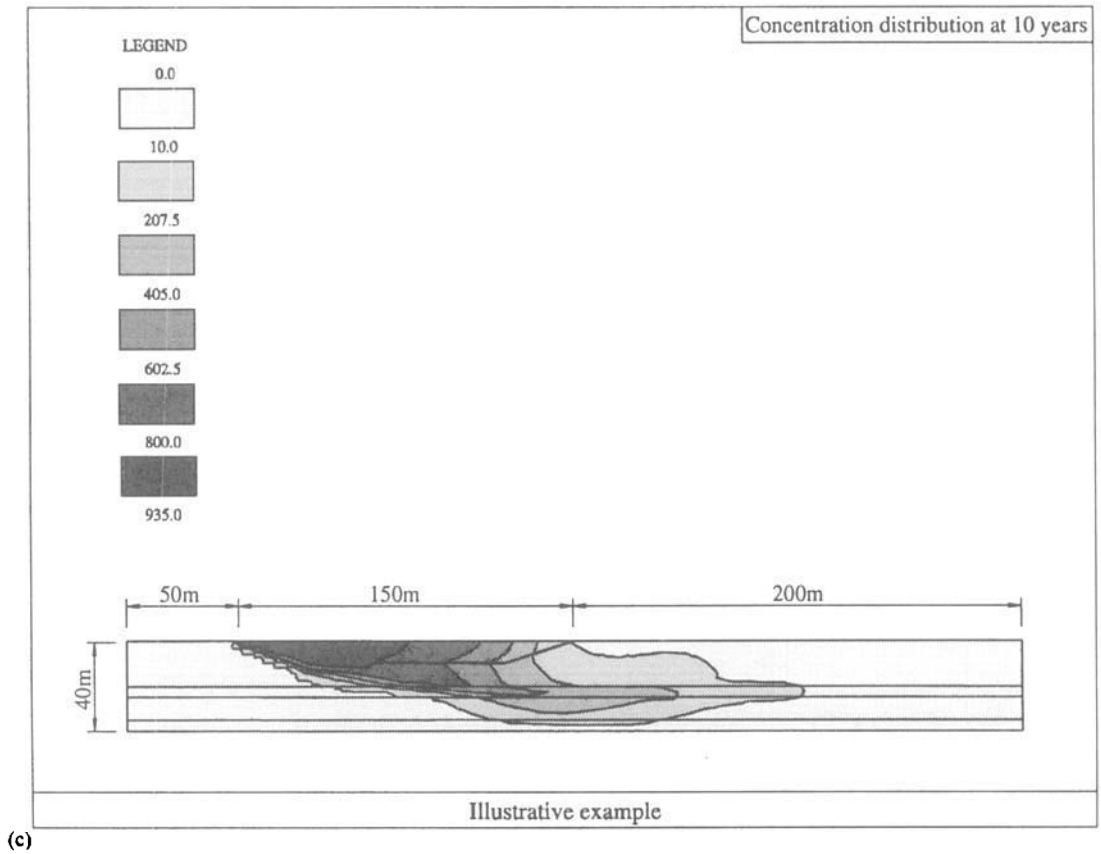

(c)

Figure 7(c). Contaminant distribution at 10 yr in illustrative example

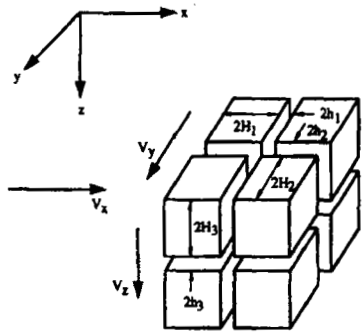

Figure 8. Fracture system in porous media (after Rowe and Booker)

APPENDIX II

In this example, the fractured material is assumed to consist of infinitely long rectangular matrix blocks separated by two sets of fractures 1 & 2 of equal spacings (i.e. $H_1 = H_2 = 0{\cdot}1$ m, $H_3 = \infty$) and the matrix properties are as follows: $n_m = 0{\cdot}1$; $D_m = 0{\cdot}003$ m^2/a, $R_m = 1$.

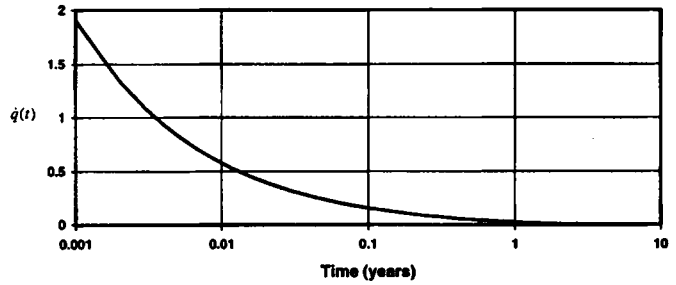

Figure 9. The function $\dot{q}(t)$ when $c_f(t) = H(t)$

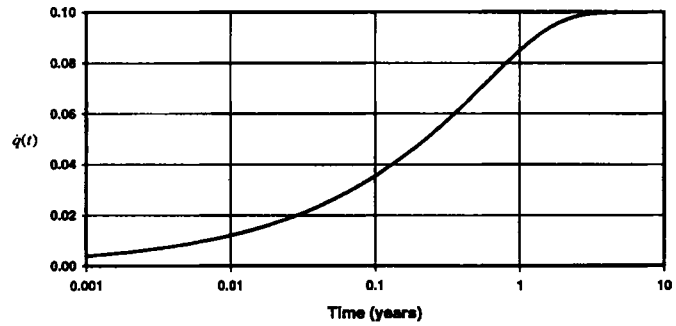

Figure 10. The function $\dot{q}(t)$ when $c_f(t) = t$

The function $\eta(t)$ for an infinitely long rectangular matrix block is given in equation (28). $\dot{q}(t)$ will depend on how $c_f(t)$ varies with time and can therefore be quite complex. Two relatively simple cases are discussed here. In the simplest case, where the concentration is initially at equilibrium and the concentration in the fracture is increased instantaneously by unit value at $t = 0$, then held constant throughout (i.e. $c_f(t) = H(t)$), it follows from equation (1) that

$$\dot{q}(t) = \eta(t) \tag{30}$$

The function $\dot{q}(t)$ for the case is shown in Figure 9. A more complex situation will be when equilibrium concentration is zero everywhere initially and then $c_f(t)$ increases linearly at unit rate (i.e. $c_f(t) = t$). It may then be shown that

$$\dot{q}(t) = \int_0^t \eta(\tau)\,\mathrm{d}\tau \tag{31}$$

this case being shown in Figure 10.

REFERENCES

1. E. A. Sudicky and R. G. McLaren, 'The Laplace transform Galerkin technique for large-scale simulation of mass transport in discretely fractured porous formations', *Water Resources Res.*, **28**, 499–514 (1992).
2. B. Berkowitz, J. Bear and C. Braester, 'Continuum models for contaminant transport in fractured porous formations', *Water Resources Res.*, **24**, 1225–1236 (1988).
3. F. W. Schwartz and L. Smith, 'A continuum approach for modeling mass transport in fractured media', *Water Resources Res.*, **24**, 1360–1372 (1988).

4. J. C. Long, J. S. Remer, C. R. Wilson and P. A. Witherspoon, 'Porous media equivalents for networks of discontinuous fractures', *Water Resources Res.*, **18**, 645–658 (1982).
5. G. de Josselin de Jong and S. C. Way, 'Dispersion in fissured rock', *Report 30*, New Mexico Inst. of Min. and Technol. Soccoro, 1972.
6. I. Neretnieks, 'Diffusion in the rock matrix: an important factor in radionuclide retardation', *J. Geophys. Res.*, **85**, 4379–4397 (1980).
7. G. E. Grisak and J. F. Pickens, 'An analytical solution for solute transport through fractured media with matrix diffusion', *J. Hydrol.* **52**, 47–57 (1981).
8. D. H. Tang, E. O. Frind and E. A. Sudicky, 'Contaminant transport in fractured porous media: analytical solution for a single fracture', *Water Resources Res.*, **17**, 555–564 (1981).
9. E. A. Sudicky and E. O. Frind, 'Contaminant transport in fractured porous media: analytical solutions of a system of parallel fractures', *Water Resources Res.*, **18**, 1634–1642 (1983).
10. A. Rasmussen, 'Migration of radionuclides in fissured rock: analytical solutions for the case of constant source strength', *Water Resources Res.*, **20**, 1435–1442 (1984).
11. D. Germain and E. O. Frind, 'Modeling contaminant migration in fracture networks: effects of matrix diffusion', in H.E. Kobus and W. Kinzelbach (eds.), *Contaminant Transport in Groundwater*, A. Balkema, Rotterdam, Netherlands 1989, pp. 267–274.
12. J. A. Barker, 'Block-geometry functions characterizing transport in densely fissured media', *J. Hydrol.* **77**, 263–279 (1985).
13. R. K. Rowe and J. R. Booker, 'A semi-analytic model for contaminant migration in a regular two- or three-dimensional fractured network: conservative contaminants', *Int. j. numer. analyt. methods geomech.*, **13**, 531–550 (1989).
14. R. K. Rowe and J. R. Booker, 'Contaminant migration in a regular two- or three-dimensional fractured network: reactive contaminants', *Int. j. numer. analyt. methods geomech.*, **14**, 401–425 (1990).
15. C. J. Leo and J. R. Booker, 'Boundary element analysis of contaminant transport in fractured porous media', *Int. j. numer. analyt. methods geomech.*, **17**, 471–492 (1993).
16. K. O'Neil and G. F. Pinder, 'A derivation of the equations for transport of liquid and heat in three dimensions in a fractured porous medium'. *Advanced Water Resources.* **4**(4), pp. 150–164.
17. A. E. Scheidegger, 'General theory of dispersion in porous media, *J. Geophys. Res.*, **66**, 3273–3278 (1961).
18. J. Bear, *Hydraulics of Groundwater*, McGraw-Hill, New York, 1979.
19. A. R. Freeze and J. A. Cherry *Groundwater*, Prentice-Hall, Englewood Cliffs, NJ, 1979.
20. O. C. Zienkiewicz and R. L. Taylor, *The Finite Element Method*, McGraw-Hill, London, 1989.
21. E. Moore, 'Exponential fitting using integral equations', *Int. j. numer. methods eng.*, **8**, 271–276 (1974).
22. A. Talbot, 'The accurate numerical integration of Laplace transforms', *J. Inst. Math. Appl.* **23**, 97–120 (1979).
23. J. R. Booker and N. P. Balaam, 'Program FESEP—steady state seepage analysis', Department of Civil Engineering, University of Sydney.
24. T. C. Rasmussen and D. D. Evans, 'Fluid flow and solute transport modeling in three-dimensional networks of variably saturated discrete fractures', *Report NUREG/CR-5239*, U.S. Nuclear Regul. Comm. Washington, DC, 1989.